Editors' Suggestion | Featured in Physics

Laser Excitation of the ^{229}Th Nuclear Isomeric Transition in a Solid-State Host

R. Elwell,[1] Christian Schneider,[1] Justin Jeet,[1] J. E. S. Terhune,[1] H. W. T. Morgan,[2] A. N. Alexandrova,[2] H. B. Tran Tan,[3,4] Andrei Derevianko,[3] and Eric R. Hudson[1,5,6]

[1]*Department of Physics and Astronomy, University of California, Los Angeles, California 90095, USA*
[2]*Department of Chemistry and Biochemistry, University of California, Los Angeles, Los Angeles, California 90095, USA*
[3]*Department of Physics, University of Nevada, Reno, Nevada 89557, USA*
[4]*Los Alamos National Laboratory, P.O. Box 1663, Los Alamos, New Mexico 87545, USA*
[5]*Challenge Institute for Quantum Computation, University of California Los Angeles, Los Angeles, California 90095, USA*
[6]*Center for Quantum Science and Engineering, University of California Los Angeles, Los Angeles, California 90095, USA*

(Received 22 March 2024; revised 19 April 2024; accepted 17 May 2024; published 2 July 2024)

$LiSrAlF_6$ crystals doped with ^{229}Th are used in a laser-based search for the nuclear isomeric transition. Two spectroscopic features near the nuclear transition energy are observed. The first is a broad excitation feature that produces redshifted fluorescence that decays with a timescale of a few seconds. The second is a narrow, laser-linewidth-limited spectral feature at $148.382\,19(4)_{\mathrm{stat}}(20)_{\mathrm{sys}}$ nm [$2020\,407.3(5)_{\mathrm{stat}}(30)_{\mathrm{sys}}$ GHz] that decays with a lifetime of $568(13)_{\mathrm{stat}}(20)_{\mathrm{sys}}$ s. This feature is assigned to the excitation of the ^{229}Th nuclear isomeric state, whose energy is found to be $8.355\,733(2)_{\mathrm{stat}}(10)_{\mathrm{sys}}$ eV in ^{229}Th:$LiSrAlF_6$.

DOI: 10.1103/PhysRevLett.133.013201

The nuclear isomeric state in the ^{229}Th nucleus, described by the Nilsson quantum numbers $(3/2)^+[631]$ has the lowest energy of all known nuclear excited states. This extraordinary property, coupled with its expected long lifetime, should allow access to a number of novel applications, including construction of an optical nuclear clock [1,2] that may be more robust and portable [3,4] than and/or outperform [5] current technology. It is also expected to allow the most sensitive test to date of the variation of the fundamental constants [4,6,7].

While recent work has greatly improved the knowledge of the isomeric state energy [8–12], to realize the aforementioned goals requires an energy measurement with laser spectroscopic precision of the isomeric transition, $(3/2)^+[631] \leftarrow (5/2)^+[633]$. It was proposed [4] that due to the optical Mößbauer effect [1,13], a high-band-gap crystal doped with ^{229}Th might provide an attractive platform for performing this spectroscopy. As a result, considerable effort has been put toward developing high-quality ^{229}Th-doped crystals, both by traditional methods [14] and using implantation at a radioactive beamline [11]. This led to an important experiment at ISOLDE [11], which established that detection of a long-lived nuclear decay ($\tau \sim 1000$ s) is possible in a crystalline host and that the wavelength of the isomeric transition was 148.7(4) nm—parentheses denotes the 68% confidence interval.

Here, we report the results of a laser-based search for the ^{229}Th isomeric nuclear transition in ^{229}Th-doped $LiSrAlF_6$ crystals. Using a vacuum-ultraviolet (VUV) laser system [15], we have searched for the transition between 147.43 nm–182.52 nm (6.793 eV–8.410 eV). We observe wideband fluorescence from ^{229}Th-doped crystals in the spectral region identified by the ISOLDE experiment [11], while undoped and ^{232}Th-doped crystals do not exhibit similar fluorescence. This fluorescence appears to possess multiple timescales that are on the order of a few seconds. We also observe a narrow, laser-linewidth-limited spectral feature at $148.382\,19(4)_{\mathrm{stat}}(20)_{\mathrm{sys}}$ nm, which decays with a lifetime of $568(13)_{\mathrm{stat}}(20)_{\mathrm{sys}}$ s. This feature does not appear in a ^{232}Th-doped $LiSrAlF_6$ crystal.

Very recently, using the approach of Ref. [4], a narrow spectroscopic feature was observed in the laser spectroscopy of ^{229}Th-doped CaF_2 crystals at 148.3821(5) nm [12]. Since this feature did not appear in a ^{232}Th-doped CaF_2 crystal it was assigned to the ^{229}Th isomeric transition. Such assignment relies on the chemical identity of ^{232}Th- and ^{229}Th-doped crystals, which, given that the radioactivity of ^{229}Th may lead to formation of radiation-induced color centers in ^{229}Th-doped crystals, is not guaranteed—especially given the history of the search for the isomeric transition using other methods [16,17]. However, given that the feature is observed in both ^{229}Th-doped CaF_2 and $LiSrAlF_6$ crystals under different experimental conditions, it appears safe to assign it to the ^{229}Th nuclear isomeric transition.

To interpret these results, we present *ab initio* crystal structure calculations that suggest the observed short-time fluorescence could be due to coupling of the ^{229}Th nucleus to the electronic and phononic degrees of freedom of the crystal. This coupling may also explain why only a fraction of the ^{229}Th nuclei doped into the crystal appear to contribute to the observed narrow, isomeric transition.

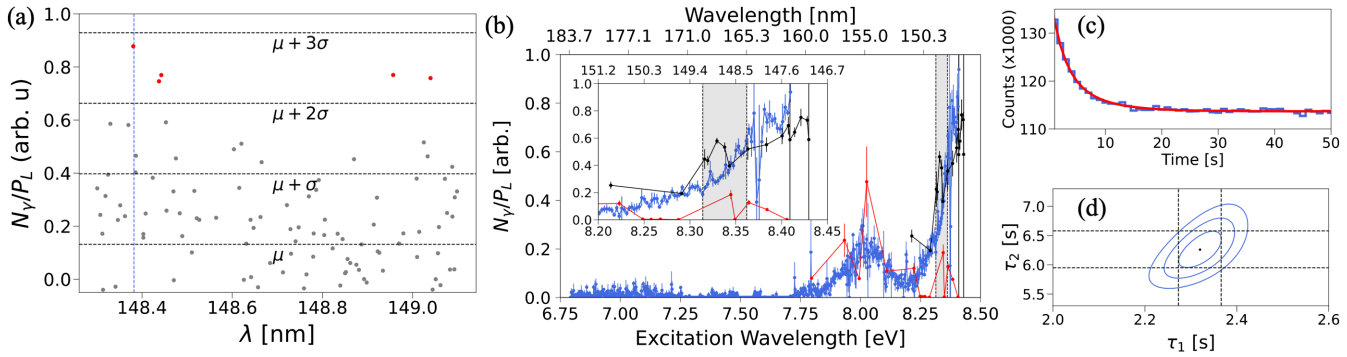

FIG. 1. (a) Long timescale fluorescence from ^{229}Th:LiSrAlF$_6$ crystal 2.2 normalized by laser power after ≈2000 s illumination shown over the 68% confidence interval of the ISOLDE experiment [11]. Dotted black lines denote the mean (μ) and mean plus multiples of the standard deviation (σ). Though the expected signal is roughly 2 orders of magnitude larger than what is observed, points above $\mu + 2\sigma$ were denoted as potential detection events and slated for further study. The vertical blue dashed line denotes the location of the narrow feature observed in Fig. 3(a). (b) Short timescale fluorescence normalized by laser power vs excitation energy in ^{229}Th (2.2 in blue, 3.1 in black) and ^{232}Th (red) LiSrAlF$_6$ crystals. The inset shows the region near the ISOLDE 68% confidence region (shaded). Each of the blue data points required roughly 1 h to collect. The drop in signal near 8.37 eV is due to a resonance in the Xe gas used for generating the VUV. (c) Time binned histogram of the short time fluorescence from ^{229}Th crystal 2.2 fitted with a two-timescale exponential decay model. (d) The likelihood contours of the two timescales found from the data in (c). Each contour represents the [68%, 95%, 99.7%] confidence regions around χ^2_{min}.

The experiments reported here were conducted via monitoring the resulting fluorescence from crystals following illumination with a VUV laser. Three different VUV transparent LiSrAlF$_6$ crystals were used in these experiments, all with dimensions ≈3 mm × 3 mm × 10 mm. Two were doped with ^{229}Th [crystal 2.2 with ^{229}Th density $\rho_{229} \approx 5(10^{16})$ cm^{-3} and crystal 3.1 with $\rho_{229} \approx 5(10^{15})$ cm^{-3}], and one was doped with ^{232}Th [$\rho_{232} \approx 1(10^{16})$ cm^{-3}] to understand any fluorescence resulting from the chemistry of Th in LiSrAlF$_6$.

VUV radiation was produced via resonance-enhanced four-wave mixing of two pulsed dye lasers (∼10 ns pulse length) in Xe gas [15,18]. The frequency of the first pulsed dye laser ω_u was locked to the $5p^6 {}^1S_0 \rightarrow 5p^5(^2P^\circ_{3/2})6p^2[1/2]_0$ two-photon transition of Xe. The frequency of the second pulsed dye laser, ω_v, was scanned to produce VUV radiation in the Xe cell given by the difference mixing relation $\omega = 2\omega_u - \omega_v$. All three laser beams then impinge on an off-axis MgF$_2$ lens, whose chromatic dispersion is used with downstream pinholes to spatially filter the VUV beam and pass it toward the crystal chamber. The laser system delivers 30 pulses per second to the crystal with a typical VUV pulse energy of ∼1 μJ/pulse and a beam diameter of roughly 2 mm (see Refs. [15,19] for details). The linewidth of this laser is estimated to be approximately 10–15 GHz based on the linewidths of the pulsed dye lasers; this width is consistent with observed absorption of the VUV when in the vicinity of Xe resonances.

The crystal under study is held in a vacuum chamber consisting of a crystal mount, two VUV-sensitive photomultiplier tubes (PMTs) (Hamamatsu R6835/R6836), and a pneumatic shutter system to protect the PMTs from direct exposure to the VUV laser. The PMTs are operated in a cathode-grounded configuration, and their output waveforms recorded by a 1 Gs/s waveform digitizer (CAEN DT5751) for subsequent postprocessing. The VUV laser beam terminates on a custom VUV energy detector. The crystal chamber is maintained with an Ar atmosphere at a pressure of ∼10^{-2} mbar to provide high VUV transmission while minimizing browning of optics due to hydrocarbon deposition [15].

Following the study reported in Ref. [19], a three-year scan was conducted with crystal 2.2 that was designed to search for crystal fluorescence with a lifetime of ≈1000 s, as would be expected for radiative relaxation of the isomeric level in a ^{229}Th:LiSrAlF$_6$ crystals [20]. For this experiment, crystal 2.2 was illuminated by VUV radiation for roughly 2000 s, the shutters were opened within 0.5 s, and any resulting fluorescence collected by the PMTs for roughly 1000 s.

For each data point constituting 2000 s of illumination, the VUV laser frequency was swept 8 times over ∼160 GHz. Each subsequent data point was then overlapped in frequency by ∼40 GHz with the previous one. This procedure was employed to minimize the probability of failing to illuminate the isomeric transition due to, e.g., multimode behavior of the pulsed dye lasers without requiring impractical data collection times.

Figure 1(a) shows the number of detected photons after background correction (N_γ) normalized by the VUV laser power (P_L) over the ISOLDE-identified 68% confidence interval [11]. The expected signal, assuming that all doped ^{229}Th nuclei are optically addressable, is roughly 2 orders of magnitude higher than the observed level. However, by analyzing the distribution of the detected photons, points

deviating from the sample mean by more than two sample standard deviations were flagged for further study, as described later.

In contrast, a clear excess of detected photons can be seen in the blue dataset of Fig. 1(b), which shows N_γ/P_L in the first 50 s after the laser is extinguished as a function of excitation wavelength. This fluorescence appears to grow considerably as the excitation wavelength approaches the region identified by the ISOLDE experiment [11]. Analysis suggests that this fluorescence possesses multiple timescales and is reasonably fit by a two-lifetime model as shown in Fig. 1(c); the likelihood contours for these two lifetimes are shown in Fig. 1(d).

Following this observation, several additional experiments were performed to ascertain the origin of the short-timescale fluorescence. For these experiments, the crystals were illuminated by the VUV laser for 60 s, the shutters opened in 100 ms, and the resulting fluorescence observed for roughly 60 s. First, a second ^{229}Th:LiSrAlF$_6$ crystal (batch 3.1) was investigated to confirm the existence of the spectral feature. The resulting fluorescence is shown as the black line in Fig. 1(b) and follows closely the observed fluorescence in crystal 2.2; the fluorescence exhibits a two-timescale behavior that is indistinguishable from that of crystal 2.2. Following these measurements, the experiment was repeated with a ^{232}Th:LiSrAlF$_6$ crystal (red line). As can be seen in Fig. 1(b), the ^{232}Th:LiSrAlF$_6$ and ^{229}Th:LiSrAlF$_6$ crystals yield a similar spectroscopic feature around 8 eV, but only the ^{229}Th:LiSrAlF$_6$ crystals yield a significant signal near the nuclear transition. Assuming this feature arises from nuclear excitation, we estimate from the known ^{229}Th density in these crystals [19] and the detection efficiency of the system that only a portion of order 1 ppm of the doped ^{229}Th atoms participate in this short-timescale process. Other explanations, such a radiation-induced color centers cannot be ruled out.

These data suggest the observed short-timescale fluorescence could have a nuclear origin and it is therefore interesting to determine the wavelength of emission. However, the number of emitted photons was sufficiently small ($\sim 10^4$ photons into 4π) that it could not be analyzed with available monochromators. Therefore, in order to determine the spectrum of the fluorescence emitted from the highest activity ^{229}Th:LiSrAlF$_6$ crystal (crystal 2.2), the transmission of the fluorescence was measured through a set of bandpass filters. An imaging system was used to collimate the collected light before passing through the filters in order to eliminate angle effects [21]. The filtered light was then focused onto a photomultiplier tube for detection. The VUV laser wavelength was chosen to be $\approx$147.4 nm to maximize the amount of fluorescence. The resulting fluorescence through various filter configurations is plotted in Fig. 2, where the horizontal axis is the central transmission wavelength of each configuration and the horizontal "error bar" denotes the FWHM of the filter

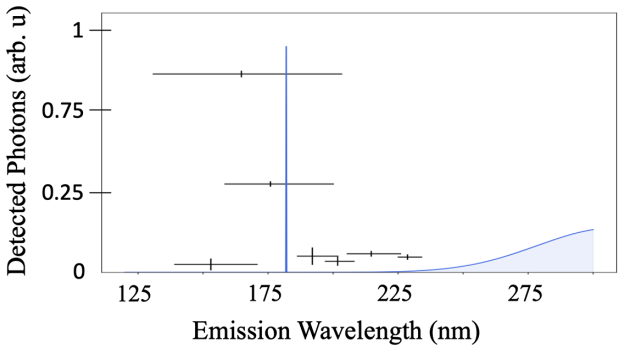

FIG. 2. Fitted spectrum for the fluorescence from crystal 2.2 under excitation at 147.4 nm using a Gaussian deconvolution (see Supplemental Material [22]). The black points represent the recorded photon numbers; the vertical line represents the statistical uncertainty while the horizontal line represents the full width at half maximum (FWHM) of the transfer function of that particular filter configuration. Each point is centered at the peak of the transfer function. The shaded blue region represents the spectrum inferred from the Gaussian deconvolution. The feature near 182 nm has a width of $\lesssim$1 nm.

transmission (see Supplemental Material [22]). As can be seen, the fluorescence is clearly in the VUV region as it primarily transmits through only two filters nominally centered at 154 nm and 180 nm. To better determine the wavelength of the emitted light, a Gaussian deconvolution procedure [23] was used to fit a model spectrum to the data (see Supplemental Material [22]). This analysis is most consistent with a narrow emission at $\approx$182 nm with a long-tailed background centered red of 280 nm. The long tail in the UV is expected and has previously been understood as due to fluorescence induced by radioactive decay of the ^{229}Th in the crystal (see Fig. 2(b) of Ref. [19]). As will be discussed later, the narrow VUV emission could be attributed to the isomeric state quenched by excitation of a defect electron-hole pair in the crystal.

Following this study of the short-timescale fluorescence, we returned to the study of the long-timescale fluorescence. The results of the ISOLDE experiment suggested that only a few percent of the ^{229}Th atoms implanted into the crystal contributed to the radiative signal [11]. This suggests that some lattice sites are quenched by coupling to the electronic structure of the crystal. Therefore, we began a new search, optimized for detection of the isomeric transition, assuming only a few percent of the doped ^{229}Th atoms contributed. This search was performed over the spectral regions within the ISOLDE region that showed an excess of photon counts relative to their neighbors [see Fig. 1(a)]. The results of that optimized search near a region of excess photons counts in our 2019 data [see dashed blue line in Fig. 1(a)], are shown in Fig. 3(a). Here, each point represents the collected long-lifetime fluorescence in 1800 s, following 1200 s of laser illumination at the given laser frequency. The total power-normalized, long-timescale fluorescence observed in this region reveals a narrow spectral feature at

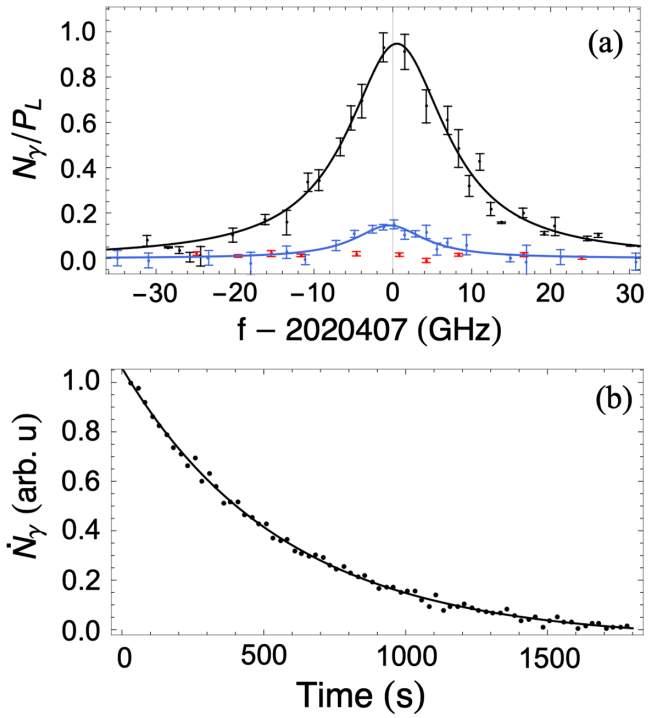

FIG. 3. (a) Spectrum of the ^{229}Th isomeric transition. The total power-normalized photon count in 1800 s following illumination is plotted versus excitation wavelength for crystal 2.2 (blue), 3.1 (black), and a ^{232}Th:LiSrAlF$_6$ crystal (red). The solid lines represent fits of a Lorentzian line shape, which result in statistically identical center frequencies. The linewidth of the fitted Lorentzians are also statistically identical and consistent with the linewidth of the VUV laser system, indicating a narrow line. (b) Observed photon count rate versus time from crystal 3.1 alongside a decaying exponential fit which determines the isomeric state lifetime within the crystal to be $\tau = 568(13)_{\mathrm{stat}}(20)_{\mathrm{sys}}$ s. A statistically identical lifetime is observed in crystal 2.2.

148.382 19$(4)_{\mathrm{stat}}(20)_{\mathrm{sys}}$ nm in both crystals 2.2 and 3.1; the primary source of systematic uncertainty is wave meter calibration (see Supplemental Material [22]). The full width at half maximum (FWHM) of this feature is roughly 15 GHz and in agreement with a measurement of the laser linewidth. The central wavelength of this feature is identical, within error, in both crystals 2.2 and 3.1 and to that observed in Ref. [12]. It is, thus, attributed to the excitation of the ^{229}Th isomeric state. From this data, we estimate that approximately 1% (50%) of the doped ^{229}Th nuclei in crystal 2.2 (3.1) are able to be excited on the nuclear isomeric transition.

The measured isomeric decay lifetime is $\tau = 568(13)_{\mathrm{stat}}(20)_{\mathrm{sys}}$ s as shown in Fig. 3(b), where the systematic error is estimated based on long-term drifts in the PMTs background count rates. The LiSrAlF$_6$ index of refraction is not well characterized in the VUV but can be estimated as 1.485 [15], leading to an estimate of the isomeric lifetime in vacuum of $\tau_{is} \approx 1860(43)_{\mathrm{stat}}(66)_{\mathrm{sys}}$ s [24]. This estimate is smaller than that observed in

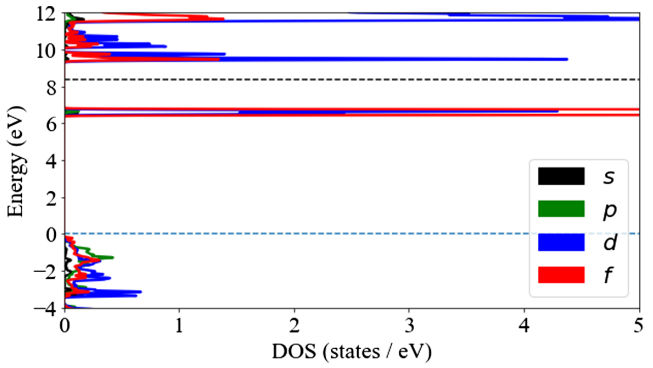

FIG. 4. Thorium PDOS for ^{229}Th:LiSrAlF$_6$. The dashed black line represents the energy of the ^{229}Th nuclear excited state relative to the top of the valence band.

^{229}Th:CaF$_2$ [12] [2510(72) s], and is likely attributed to a poor estimate of the index of refraction of these crystals in the VUV, though other explanations are discussed later. Nonetheless, both values are within the range predicted in Ref. [20].

To better understand these results, we performed density functional theory (DFT) calculations using the modified Becke-Johnson [25,26] functional to estimate the electronic properties of the ^{229}Th-doped crystals (see Supplemental Material [22]). Figure 4 shows the projected density of states (PDOS) for Th in Th:LiSrAlF$_6$, in a $3 \times 3 \times 2$ supercell containing one Th atom and two interstitial F atoms for charge balancing; this is the lowest-energy configuration in our calculations (see Supplemental Material [22]). We find a manifold of the Th $5f$ states at 6.8 eV (182 nm) inside the insulator band gap (d_i states). This is consistent with the observed fluorescence wavelength in Fig. 2, indicating the possibility of nuclear decay via excitation of a valence-band electron to a d_i state. Subsequent photon emission via the recombination of the d_i state with the hole, which has moved to the top of the valence band on picosecond timescales typical for non-radiative relaxation of hot holes [27], would produce the observed, redshifted 182 nm photons.

Such coupling of the electron and nuclear subsystems is mediated by the hyperfine interaction (HFI). In the absence of the HFI, the eigenstates of the system are the product states $|\mathrm{el}\rangle|\mathrm{nuc}\rangle$; the HFI leads to admixtures of the excited nuclear state $|e\rangle$ with the product states involving the ground $|g\rangle$ nuclear state. In the first part of the process, the laser excites the occupied valence band state $\approx|\Omega\rangle|g\rangle$ to a particle-hole eigenstate $|\Psi_L\rangle = a^\dagger_{d_i} a_h|\Omega\rangle|g\rangle + |\delta\Phi_{\mathrm{el}}\rangle|e\rangle$ resonant with the laser frequency (here, we use the creation and annihilation operators $a^\dagger$ and a; $|\Omega\rangle$ is the valence band quasivacuum state). The HFI-mediated admixture $|\delta\Phi_{\mathrm{el}}\rangle|e\rangle$ can be substantial due to a contribution of the $a^\dagger_{d_i} a_{h_r}|\Omega\rangle$ states resonant with the nuclear transition. It also contains the $|\Omega\rangle|e\rangle$ state. Such laser excitation exhibits a steplike character of Fig. 1(b). The components of this coherently excited

state decay due to a combination of vibronic couplings to the crystal on a picosecond timescale and radiative particle-hole recombination on a nanosecond timescale. While the majority of the decays result in a photon emission on the nanosecond timescale, some population may evolve into the state $|\Omega\rangle|e\rangle$. The resulting $|\Omega\rangle|e\rangle$ state is embedded into the continuum of particle-hole states $a^\dagger_{d_i}a_h|\Omega\rangle|g\rangle$ and can thereby decay into this continuum with the rate $\Gamma = 2\pi\rho|\langle e|\langle\Omega|V_{\mathrm{HFI}}|a^\dagger_{d_i}a_{h_r}|\Omega\rangle|g\rangle|^2$. Here, the hole h_r is such that the energy difference $\varepsilon_{d_i} - \varepsilon_{h_r}$ matches the nuclear excitation energy ω_{nuc} and ρ is the valence band density of states. The rate has to be summed over all allowed final states, including phonon degrees of freedom which bring in Frank-Condon factors in the rate evaluation. This internal conversion process quenches the nuclear transition. The vibronic couplings further "float" the hot resonant hole state h_r to the top of the valence band. Finally, a radiative particle-hole recombination emits a fluorescence photon that is redshifted compared to ω_{nuc}. We find that this model semiquantitatively explains the observed short-timescale fluorescence spectrum of Figs. 1(b)–1(d) and 2; full numerical simulations will be reported elsewhere.

This mechanism relies on the energy of the $5f$ defect states ε_{d_i} being lower than ω_{nuc}. Thus, the long-timescale signal observed from the nuclear isomeric transition is potentially due to ^{229}Th atoms that are substituted into the crystal in arrangements that have $\varepsilon_{d_i} > \omega_{\mathrm{nuc}}$ or vanishing ρ near the isomeric energy. Finally, even without coupling to defect states, the nuclear radiative lifetime may still be shortened by effects of the crystal electric field, which mix Th electronic states of opposite parity. The hyperfine interaction couples the nuclear degree of freedom to these mixed-parity states, allowing for a competing $E1$ decay channel for the isomeric state. Such effects may complicate efforts to determine the radiative lifetime of the bare ^{229}Th isomeric state from that observed in crystalline hosts.

Given these results and those of Ref. [12], it is clear that the ^{229}Th isomeric transition is now measured with laser spectroscopic precision, completing the journey started by Kroger and Reich [28] nearly 50 years ago. With a narrow feature identified in two separate crystalline hosts, a number of exciting experiments and applications can be explored. These include studying the variation of the transition properties (frequency and linewidth) with chemical environment [1], cooperative nuclear spontaneous emission [29], and the construction of what may prove to be the ultimate time keeping device, the nuclear clock [4,5,30].

The authors thank Yafis Barlas, Arlete Cassanho, Yih-Chung Chang, Hans Jenssen, Saed Mirzadeh, Cheuk Ng, and Martin Pimon for valuable discussions. This work was supported by NSF Awards No. PHYS-2013011 and No. PHY-2207546, and ARO Award No. W911NF-11-1-0369. E. R. H. acknowledges institutional support by the NSF QLCI Award No. OMA-2016245. This work used Bridges-2 at Pittsburgh Supercomputing Center through allocation PHY230110 from the Advanced Cyberinfrastructure Coordination Ecosystem: Services & Support (ACCESS) program, which is supported by National Science Foundation Grants No. 2138259, No. 2138286, No. 2138307, No. 2137603, and No. 2138296.

[1] E. V. Tkalya, V. O. Varlamov, V. V. Lomonosov, and S. A. Nikulin, Phys. Scr. **53**, 296 (1996).
[2] E. Peik and C. Tamm, Europhys. Lett. **61**, 181 (2003).
[3] E. R. Hudson, A. C. Vutha, S. K. Lamoreaux, and D. DeMille, *Investigation of the Optical Transition in the 229Th Nucleus: Solid-State Optical Frequency Standard and Fundamental Constant Variation, Poster MO28, International Conference on Atomic Physics* (2008).
[4] W. G. Rellergert, D. DeMille, R. R. Greco, M. P. Hehlen, J. R. Torgerson, and E. R. Hudson, Phys. Rev. Lett. **104**, 200802 (2010).
[5] C. J. Campbell, A. G. Radnaev, A. Kuzmich, V. A. Dzuba, V. V. Flambaum, and A. Derevianko, Phys. Rev. Lett. **108**, 120802 (2012).
[6] V. V. Flambaum, Phys. Rev. Lett. **97**, 092502 (2006).
[7] E. Litvinova, H. Feldmeier, J. Dobaczewski, and V. Flambaum, Phys. Rev. C **79**, 064303 (2009).
[8] L. von der Wense, B. Seiferle, M. Laatiaoui, J. B. Neumayr, H.-J. Maier, H.-F. Wirth, C. Mokry, J. Runke, K. Eberhardt, C. E. Düllmann *et al.*, Nature (London) **533**, 47 (2016).
[9] B. Seiferle, L. von der Wense, P. V. Bilous, I. Amersdorffer, C. Lemell, F. Libisch, S. Stellmer, T. Schumm, C. E. Düllmann, A. Pálffy, and P. G. Thirolf, Nature (London) **573**, 243 (2019).
[10] T. Sikorsky, J. Geist, D. Hengstler, S. Kempf, L. Gastaldo, C. Enss, C. Mokry, J. Runke, C. E. Düllmann, P. Wobrauschek *et al.*, Phys. Rev. Lett. **125**, 142503 (2020).
[11] S. Kraemer, J. Moens, M. Athanasakis-Kaklamanakis, S. Bara, K. Beeks, P. Chhetri, K. Chrysalidis, A. Claessens, T. E. Cocolios, J. G. M. Correia *et al.*, Nature (London) **617**, 706 (2023).
[12] J. Tiedau, M. V. Okhapkin, K. Zhang, J. Thielking, G. Zitzer, E. Peik, F. Schaden, T. Pronebner, I. Morawetz, L. Toscani De Col *et al.*, Phys. Rev. Lett. **132**, 182501 (2024).
[13] E. V. Tkalya, A. N. Zherikhin, and V. I. Zhudov, Phys. Rev. C **61**, 064308 (2000).
[14] K. Beeks, T. Sikorsky, V. Rosecker, M. Pressler, F. Schaden, D. Werban, N. Hosseini, L. Rudischer, F. Schneider, P. Berwian *et al.*, Sci. Rep. **13**, 3897 (2023).
[15] J. Jeet, Search for the low lying transition in the ^{229}Th nucleus, Ph.D. thesis, University of California, Los Angeles, 2018, https://escholarship.org/uc/item/8wk771ch.
[16] G. M. Irwin and K. H. Kim, Phys. Rev. Lett. **79**, 990 (1997).
[17] R. W. Shaw, J. P. Young, S. P. Cooper, and O. F. Webb, Phys. Rev. Lett. **82**, 1109 (1999).
[18] M. Berdah, J. Visticot, C. Dedonder-Lardeux, D. Solgadi, and B. Soep, Opt. Commun. **124**, 118 (1996).
[19] J. Jeet, C. Schneider, S. T. Sullivan, W. G. Rellergert, S. Mirzadeh, A. Cassanho, H. P. Jenssen, E. V. Tkalya, and E. R. Hudson, Phys. Rev. Lett. **114**, 253001 (2015).

[20] E. V. Tkalya, C. Schneider, J. Jeet, and E. R. Hudson, Phys. Rev. C **92**, 054324 (2015).
[21] M. Lödahl, V. M. J. Henriques, and D. Kiselman, Astron. Astrophys. **533**, A82 (2011).
[22] See Supplemental Material at http://link.aps.org/supplemental/10.1103/PhysRevLett.133.013201 for further details of the experiment, data processing, and crystal structure calculations.
[23] G. H. Major, N. Fairley, P. M. A. Sherwood, M. R. Linford, J. Terry, V. Fernandez, and K. Artyushkova, J. Vac. Sci. Technol. A **38**, 061203 (2020).
[24] E. Tkalya, JETP Lett. **71**, 311 (2000).
[25] F. Tran and P. Blaha, Phys. Rev. Lett. **102**, 226401 (2009).
[26] A. D. Becke and E. R. Johnson, J. Chem. Phys. **124**, 221101 (2006).
[27] M. Woerner, T. Elsaesser, and W. Kaiser, Phys. Rev. B **45**, 8378 (1992).
[28] L. Kroger and C. Reich, Nucl. Phys. **A259**, 29 (1976).
[29] E. V. Tkalya, Phys. Rev. Lett. **106**, 162501 (2011).
[30] Y. Shvyd'ko *et al.*, Nature (London) **622**, 471 (2023).